Available online at www.sciencedirect.com

ScienceDirect

www.elsevier.com/locate/jes

JES JOURNAL OF ENVIRONMENTAL SCIENCES

www.jesc.ac.cn

Effects of O_3/Cl_2 disinfection on corrosion and opportunistic pathogens growth in drinking water distribution systems

Haibo Wang[1], *Chun Hu*[1,2,3,*], *Suona Zhang*[1,3], *Lizhong Liu*[1,3], *Xueci Xing*[1,3]

1. *Key Laboratory of Drinking Water Science and Technology, Research Center for Eco-Environmental Sciences, Chinese Academy of Sciences, Beijing 100085, China. E-mail: hbwang@rcees.ac.cn*
2. *Research Institute of Environmental Studies at Greater Bay, School of Environmental Sciences and Engineering, Guangzhou University, Guangzhou 510006, China*
3. *University of Chinese Academy of Sciences, Beijing 100049, China*

ARTICLE INFO

Article history:
Received 19 September 2017
Revised 11 January 2018
Accepted 11 January 2018
Available online 3 February 2018

Keywords:
Ozone
Chlorine
Corrosion
Opportunistic pathogens
Drinking water distribution systems

ABSTRACT

The effects of O_3/Cl_2 disinfection on corrosion and the growth of opportunistic pathogens in drinking water distribution systems were studied using annular reactors (ARs). The corrosion process and most probable number (MPN) analysis indicated that the higher content of iron-oxidizing bacteria and iron-reducing bacteria in biofilms of the AR treated with O_3/Cl_2 induced higher Fe_3O_4 formation in corrosion scales. These corrosion scales became more stable than the ones that formed in the AR treated with Cl_2 alone. O_3/Cl_2 disinfection inhibited corrosion and iron release efficiently by changing the content of corrosion-related bacteria. Moreover, ozone disinfection inactivated or damaged the opportunistic pathogens due to its strong oxidizing properties. The damaged bacteria resulting from initial ozone treatment were inactivated by the subsequent chlorine disinfection. Compared with the AR treated with Cl_2 alone, the opportunistic pathogens *M. avium* and *L. pneumophila* were not detectable in effluents of the AR treated with O_3/Cl_2, and decreased to (4.60 ± 0.14) and (3.09 ± 0.12) $\log_{10}$ (gene copies/g corrosion scales) in biofilms, respectively. The amoeba counts were also lower in the AR treated with O_3/Cl_2. Therefore, O_3/Cl_2 disinfection can effectively control opportunistic pathogens in effluents and biofilms of an AR used as a model for a drinking water distribution system.

Introduction

The opportunistic pathogens in drinking water distribution systems (DWDSs) present an emerging health risk to humans, especially immunocompromised populations (Thomas and Ashbolt, 2011). Recently, opportunistic pathogens including *Legionella pneumophila*, *Mycobacterium avium*, *Pseudomonas aeruginosa*, and the free-living amoeba, such as *Acanthamoeba* spp. and *Naegleria fowleri*, have been found in DWDSs and tap water (Campese et al., 2011; Wang et al., 2013; Morgan et al., 2016). Tap water is a direct route for human exposure to opportunistic pathogens, typically by inhalation of aerosols or skin contact (Wang et al., 2012a). Amoebae can slough off or migrate into the bulk water from biofilms and make their way into contact with humans through the DWDSs (Miller et al., 2015; Morgan et al., 2016).

* *Corresponding author. E-mail:* huchun@rcees.ac.cn (Chun Hu).

https://doi.org/10.1016/j.jes.2018.01.009
1001-0742/

Bacterial growth in DWDSs includes regrowth in bulk water and formation of biofilms (Langmark et al., 2007; Liu et al., 2014). Biofilms in DWDSs provide microenvironments for opportunistic pathogen growth (Berry et al., 2006). Moreover, biofilms are always formed in the corrosion scales of metal pipes (Wang et al., 2014). Gomez-Smith et al. (2015) have found many opportunistic pathogens, such as *M. avium*, in the biofilms of corrosion scales. The opportunistic pathogens in biofilms can release into the bulk water during metal release from corrosion scales, resulting in higher numbers of opportunistic pathogens in the bulk water of DWDSs with iron pipes compared to those with PVC pipes (Wang et al., 2012b). Yang et al. (2012) have indicated that thick and densely distributed corrosion scales with higher Fe_3O_4 content are more stable, and thin corrosion scales with higher α-FeOOH and $FeCO_3$ content more easily release iron into the distributed water. More iron release will result in discoloration of tap water, leading to customer complaints (Li et al., 2010). Therefore, both the iron release and opportunistic pathogens growth will affect the bulk water quality of DWDSs.

In order to control the bacterial growth in DWDSs, the final disinfection step typically involves the addition of chlorine or chloramines, and a constant disinfectant residual concentration is also required (Hwang et al., 2012; Mi et al., 2015; Moradi et al., 2017). However, opportunistic pathogens possess several adaptive features, including resistance to disinfection and tendency to form biofilms, to aid their survival (Wang et al., 2013), and many opportunistic pathogens are found in tap water (Wang et al., 2012a; Delafont et al., 2014; Thomas et al., 2014). Therefore, more powerful disinfection technologies should be applied to control opportunistic pathogens in DWDSs. Advanced disinfection methods, including ozone, hydrogen peroxide, ultraviolet (UV) and electrochemical treatment, are promising technologies for removing microorganisms (Li et al., 2011; Sun et al., 2017). Among these advanced disinfection technologies, ozone has gained attention for inactivating microorganisms in drinking water treatment, due to its strong oxidizing properties (Gunten, 2003; Alexander et al., 2016). However, ozone also needs to be employed together with chlorine to maintain a disinfectant residual in DWDSs. Ozone followed by chlorine disinfection has been used to inactivate *Cryptosporidium parvum oocysts* and *Bacillus subtilis* spores in drinking water (Corona-Vasquez et al., 2002; Cho et al., 2003). Currently, there is little known about the effect of sequential ozone and chlorine disinfection on the opportunistic pathogens in DWDSs. Moreover, the addition of ozone to disinfection will affect the biofilms bacterial community in DWDSs, which can affect the corrosion process and iron release in DWDSs (Wang et al., 2012c). Reports about the effects of O_3/Cl_2 disinfection on the corrosion and iron release in DWDSs are also scarce.

Therefore, the objective of this study is to investigate the effects of O_3/Cl_2 disinfection on corrosion and opportunistic pathogens growth in DWDSs, with Cl_2 disinfection alone acting as a reference. The mechanism for control of iron release and opportunistic pathogens growth in DWDSs by O_3/Cl_2 disinfection is also discussed.

1. Materials and methods

1.1. Materials and model distribution systems

Two annular reactors (ARs) (Model 1320LJ, BioSurface Technologies Co., USA) were used to simulate DWDSs, as described in other studies (Murphy et al., 2008; Wang et al., 2012c). The schematic of the experimental set-up was shown in Appendix A Fig. S1. In the ARs, there were two concentric glass cylinders and a rotating inner drum that supported 20 cast iron coupons. The cast iron coupons with an elemental composition (wt%) of C 3.25%, O 1.63%, Si 2.23%, P 0.08%, S 0.10%, Fe 90.48%, Cu 0.76%, Mn 0.72%, and Zn 0.75% were used. Each coupon had an exposed surface area of 17.5 cm^2 for biofilms growth. The two ARs were arranged in parallel and operated at a rotational speed of 50 r/min, according to the conditions employed to simulate DWDSs using ARs in a previous study (Murphy et al., 2008). The hydraulic retention time (HRT) of the reactors was 6 hr, which translated to a total flow rate of 2.8 mL/min into the ARs. The HRT was also consistent with the previous study using ARs (Murphy et al., 2008).

In one AR, the test water used as influent was treated with O_3 for a contact time of 12 min in a 6-L reactor. Approximately 46 mg of gaseous O_3/L oxygen-ozone was bubbled into the reactor through a porous plate in the reactor bottom at a flow rate of 200 mL/min. The residual ozone dosage in the water was about 0.55 mg/mg dissolved organic carbon (DOC). After 2 hr, the residual ozone dosage decayed to zero. Then, the AR was exposed to chlorine as the second disinfectant. Chlorine was dosed from a stock solution of NaClO. After chlorination for 4 hr, the water was pumped into the AR. The second AR was operated with chlorine as the only disinfectant. Before day 60, the initial chlorine concentration in both ARs was 2.3 mg/L, and it was increased to 2.6 mg/L from day 60 to day 240 in order to increase the chlorine residual in the effluents of both ARs. The chlorine residual and total iron concentration in effluents of both ARs were analyzed in triplicate. The results are shown in Fig. 1.

1.2. The tested water and water quality

The tested raw water was collected from a drinking water treatment plant in north of China, which was treated with coagulation using polyaluminum chloride, sedimentation, sand filtration, and biologically-activated carbon filtration (prior to entering the chlorine contact tanks). Water quality parameters (Appendix A Table S1) were measured according to standard methods (EPA of China, 2002). pH was measured using a Mettler Toledo pH Meter (FE20K, China). The total iron concentration was analyzed by an Inductively Coupled Plasma Optical Emission Spectrometer (SHIMADZU, ICPE-9820, Japan). The initial chlorine concentration and chlorine residual were measured using a HANNA HI93711 spectrophotometer (Italy) according to the DPD (*N*, *N*-diethyl-*ρ*-phenylenediamine) colorimetric method. DOC was analyzed *via* a total organic carbon analyzer (TOC-V_{CPH}, SHIMADZU, Japan). Differences in water quality parameters between the two ARs were analyzed using analysis of variance (ANOVA) with a significance threshold of $\alpha = 0.05$.

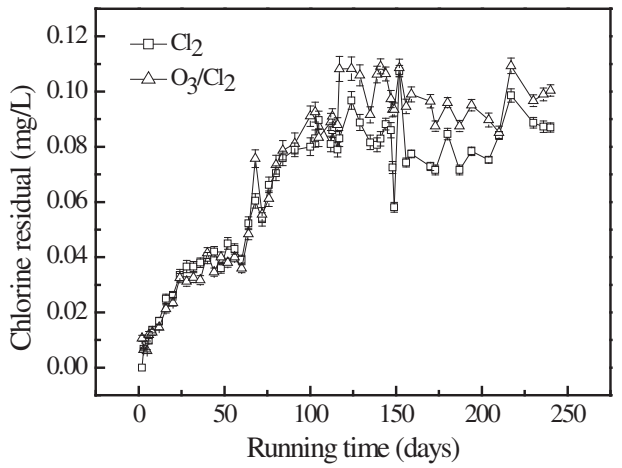

Fig. 1 – The chlorine residual in effluents of both annular reactors (ARs) treated with O_3/Cl_2 and Cl_2 alone at different running times. Error bars represent the standard deviation from the average of three replications.

1.3. Characterizing corrosion process and corrosion scales

The weight loss method was utilized to determine the corrosion rate. Briefly, the scraped coupons were rinsed with 70% ethanol, gently wiped with cotton swabs, freeze-dried for a day and weighed to determine the weight loss. The calculation method is listed in Appendix A Text S1.

After sampling, the coupons were dried by freeze-drying under vacuum conditions. Then, the corrosion scales were scraped from the surface of the coupons with a sterile razor blade for the analysis of surface characteristics. The surface characteristics and corrosion features were examined by Field Emission Scanning Electron Microscopy (FESEM) (Hitachi, SU8020). Crystalline phase composition was analyzed using an X-ray powder diffractometer (XRD, X'Pert PRO MPD; PANalytical, The Netherlands).

1.4. Sample collection, PMA treatment and DNA extraction

One-liter water samples from the influents and effluents of both ARs were filtered through 0.2-μm polycarbonate filters using a sterile filter funnel and vacuum flask setup, respectively. The filters were stored in sterile 2-mL microfuge tubes before DNA extraction. Biofilms in the corrosion scales were also collected. The corrosion scales were freeze-dried under vacuum conditions and scraped from the surface of the coupons. Then, 0.4-g samples were weighed and put into the microfuge tubes before DNA extraction.

The propidium monoazide (PMA) bound DNA cannot be amplified in the ensuing polymerase chain reactions (PCR) (Zhang et al., 2015). This characteristic is often applied to quantify the DNA of live bacteria and characterize the changes in viable bacterial communities (Chiao et al., 2014; Gensberger et al., 2014). The water and biofilms samples were subjected to PMA treatment by incubating the polycarbonate membrane filters and 0.4 g of corrosion scales in 40 μmol/L PMA solution, respectively. The process of PMA treatment of samples was described in Appendix A Text S2. The *E. coli* cells (ATCC 25922, 10^7–10^8 CFU/mL) were chosen as representative microorganisms to determine the optimal PMA concentration (Chiao et al., 2014; Gensberger et al., 2014). A range of concentrations (0, 30, 40 and 50 μmol/L PMA) was selected based on related research to maximize removal of DNA from 70%-isopropanol-killed (30 min incubation) cells while minimizing the effects on DNA from live cells harvested during the exponential growth phase. The optimum PMA concentration of 40 μmol/L was used in this study (Appendix A Fig. S2). This optimum PMA concentration of 40 μmol/L was validated on untreated (live) and isopropanol-treated (70%) (30-min incubation) (dead) cells from the effluent of DWDSs with raw water (Appendix A Fig. S3). After PMA treatment, samples were subjected to DNA extraction with the FastDNA SPIN Kit (MP Biomedicals, Solon, OH, USA) following the manufacturer's instructions. To determine the method recovery efficiency, *E. coli* was used as a representative microorganism according to our previous method (Wang et al., 2017). The recovery efficiency varied from 19.1% to 40.5% depending on the concentration of samples. DNA quality was checked on an agarose gel, and concentrations were measured with a Nanodrop spectrophotometer (ND-1000, NanoDrop, USA). All DNA samples were stored at −80°C until further processing.

1.5. Quantitative PCR

The quantitative polymerase chain reactions (qPCR) experiments were carried out with the ABI 7300 Fast Real-Time PCR System (Applied Biosystems, Singapore) using premix Ex Taq or SYBR premix Ex Taq (TaKaRa, Dalian, China) in a 25-μL reaction volume. Previously published primer sequences and qPCR methods were used to detect the 16S rRNA for total bacteria (Wang et al., 2012a, 2012b), opportunistic pathogens including *Pseudomonas aeruginosa* (Zhang et al., 2015), *Legionella pneumophila* (Wang et al., 2012a, 2012b), *Mycobacterium avium* (Wang et al., 2012a, 2012b), the broader genera *Legionella* spp. (Wang et al., 2012a, 2012b), *Mycobacterium* spp. (Wang et al., 2012a, 2012b), and the amoebae *Acanthamoeba* spp. (Wang et al., 2012a, 2012b), and *Naegleria* spp. (Thomas et al., 2014). qPCR was performed in a 25-μL final reaction mixture volume consisting of 12.5 μL of Premix Ex Taq (Takara, Dalian, China), 0.5 μL of 10 μmol/L forward and reverse primers, 1.0 μL of 3 μmol/L TaqMan probe, 8.5 μL of distilled water, 0.5 μL of ROX reference dye (50×), and 2.0 μL of DNA template. If there was no probe, 12.5 μL of SYBE Ex Taq (Takara, Dalian, China) and 9.5 μL of distilled water were used. The PCR program contained an initial 3-min denaturation step at 95°C, followed by 40 amplification cycles consisting of an initial denaturation at 95°C for 30 sec followed by 30 sec at 50–60°C for different bacteria and 30 sec at 72°C. The details of primer sequences and annealing temperatures for 16S rRNA and the different opportunistic pathogens are presented in Appendix A Table S2. The analysis procedures were described in Appendix A Text S3. Standard curves were generated by serial ten-fold dilution (10^9–10^2 copies/μL) of the plasmids. The information of average slope of the standard curve and amplification efficiency of the qPCR tests were listed in Supporting Information (Appendix A Table S3). The amplification efficiency values for quantification ranged from 95.30% to 99.79%. The limit of quantification (LOQ) for all qPCR assays ranged from 1 to 10 gene copies/reaction and was implemented as appropriate for each specific run.

1.6. Most probable number enumeration

The abundance of culturable Fe(III)-reducing bacteria (IRB) and nitrate-dependent Fe(II)-oxidizing bacteria (IOB) in the biofilms of corrosion scales from different pipes was analyzed using a three-tube most probable number (MPN) technique. Triplicate pressure tubes containing sterile, anaerobic (N_2:CO_2; 90:10, V/V) artificial ground water (AGW) medium (10 mmol/L PIPES, 2 mmol/L $NaHCO_3$, 5 mmol/L NH_4Cl, 0.5 mmol/L KH_2PO_4, pH 6.8) were inoculated with homogenized corrosion scales. For testing of the IOB and IRB in the biofilms of corrosion scales, the AGW medium was amended according to previous studies (Coby et al., 2011; Wang et al., 2017). For acetate-oxidizing Fe(III)-reducing bacteria, the medium was amended with 10 mmol/L of synthetic hydrous ferric oxide prior to autoclaving, and then amended with 10 mmol/L Na-acetate and 2 mmol/L $FeCl_2$ (as a reducing agent) from sterile, anaerobic stock solutions. The medium for Fe(II)-oxidizing nitrate-reducing bacteria was amended with 0.5 mmol/L Na-acetate, 5 mmol/L $NaNO_3$ and 10 mmol/L $FeCl_2$ from sterile, anaerobic stock solutions. Visual assessment of blackening of the medium, and formation of reddish-brown precipitates, was used to identify positive results for Fe(III) reducers and nitrate-dependent Fe(II) oxidizers, respectively.

After the MPN enumerations, the Fe(II) oxidation and Fe(III) reduction products caused by the bacterial function in biofilms were analyzed using an X-ray powder diffractometer (XRD, X'Pert PRO MPD; PANalytical, The Netherlands) to determine the crystalline phase composition.

2. Results and discussion

2.1. Chlorine residual and total iron concentration

Before day 60, the initial chlorine concentration was 2.3 mg/L in both ARs which were treated with O_3/Cl_2 disinfection or Cl_2 alone. Because chlorine reacted with the new cast iron coupons, the chlorine residual in the effluents of both ARs could hardly be detected before day 10 (Fig. 1). After that, the chlorine residual in both ARs increased with running time, and it reached a relatively stable value in both ARs at day 30. From day 30 to day 60, the chlorine residual was about 0.04 mg/L in the effluents of both ARs, and there was no significant difference between both ARs ($p = 0.07 > 0.05$). From day 60, the initial chlorine concentration was increased to 2.6 mg/L in both ARs in order to increase the chlorine residual. The chlorine residual increased and reached a relatively stable value in both ARs at day 100. From day 100 to day 250, the average chlorine residual in the AR treated with O_3/Cl_2 was 0.097 mg/L, which was higher than that (0.083 mg/L) in the AR treated with Cl_2 alone ($p < 0.05$).

Moreover, due to the rapid reaction between chlorine and the new cast iron coupons, the total iron concentrations in the effluents of both ARs were very high at day 2 (Fig. 2). The total iron concentration was 0.273 mg/L and 0.308 mg/L in the effluents of ARs treated with Cl_2 alone and O_3/Cl_2 disinfection, respectively. After that, the total iron concentration decreased with running time, and it gradually arrived at a relatively stable value from day 10 to day 50. The average total iron concentration (0.096 mg/L) in the effluents of AR treated O_3/Cl_2 was higher than that AR (0.084 mg/L) treated with Cl_2 alone ($p < 0.05$). However, from day 50 to day 60, the total iron concentration in the effluents of AR treated with O_3/Cl_2 was lower than that in the effluents of AR treated with Cl_2 alone. Moreover, from day 60 on, the initial chlorine concentration was increased from 2.3 to 2.6 mg/L, and the total iron concentration in the effluents of both ARs changed very little. From day 60 to day 250, the average total iron concentration (0.088 mg/L) in the effluents of AR treated with O_3/Cl_2 was still lower than that AR (0.104 mg/L) treated with Cl_2 alone ($p < 0.05$).

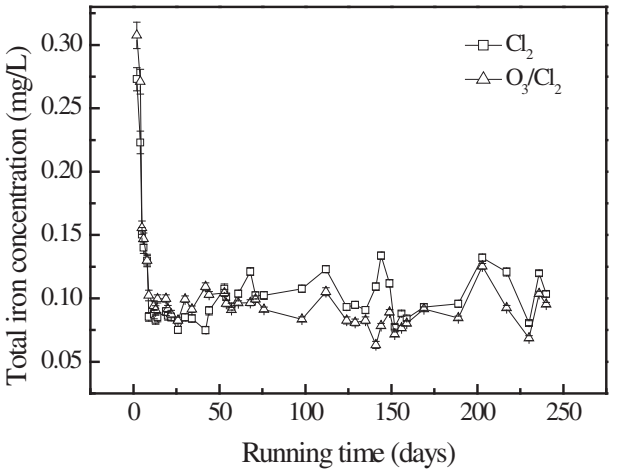

Fig. 2 – Total iron concentration in effluents of both ARs treated with O_3/Cl_2 and Cl_2 alone at different running times. Error bars represent the standard deviation from the average of three replications.

The iron release was related to the iron corrosion process and physico-chemical characteristics of corrosion scales (Sarin et al., 2001; Jin et al., 2015). Before day 10, the stable corrosion scales was not formed in both ARs, and the high iron release suggested the high corrosion rate. Therefore, during this period, the corrosion rate of cast iron coupons in AR treated with O_3/Cl_2 may be higher than that with Cl_2 alone. After day 50, the lower iron release in AR treated with O_3/Cl_2 may be caused by the formation of stable corrosion scales.

2.2. Stable corrosion scales formation in different ARs

The corrosion rate of cast iron coupons in different ARs was detected by the weight loss method. Before day 40, the corrosion rate (0.138 ± 0.004 mm/year) was higher in AR treated with O_3/Cl_2 than that of (0.125 ± 0.003 mm/year) AR treated with Cl_2 alone (Appendix A Fig. S4). From day 40 to day 170, the corrosion rate decreased in both ARs; however, it (0.076 ± 0.001 mm/year) was lower in AR treated with O_3/Cl_2 than that of AR (0.093 ± 0.001 mm/year) treated with Cl_2 alone.

The different corrosion rates may result in different corrosion scales formation. The XRD patterns showed that the main crystalline compounds were goethite (α-FeOOH) and green rust (GR, $Fe_6(OH)_{12}CO_3$) before day 40 (Fig. 3). Calcite

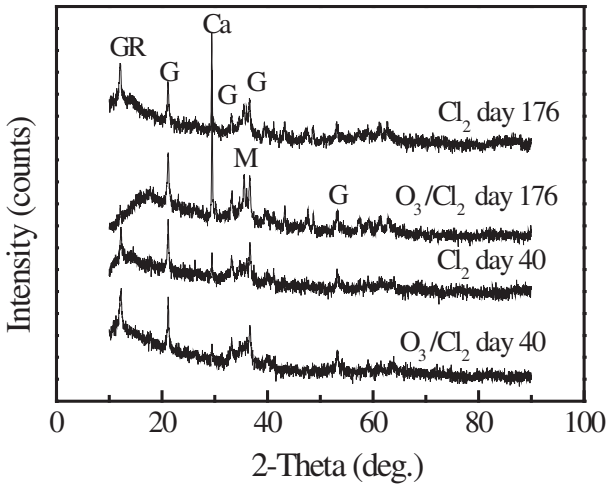

Fig. 3 – X-ray powder diffraction (XRD) patterns of the corrosion scales on the surface of cast iron coupons in ARs treated with O_3/Cl_2 and Cl_2 alone at different running times. G: goethite, GR: green rust, M: magnetite, Ca: calcite.

($CaCO_3$) was also formed in both ARs, but the peak intensity was weak. The peak intensities of $CaCO_3$ increased obviously in both ARs from day 40 to day 170. The magnetite (Fe_3O_4) was also formed in both ARs at day 170. However, the peak intensity of Fe_3O_4 in AR treated with O_3/Cl_2 was higher than that in AR treated with Cl_2 alone. Furthermore, the peak intensity of α-FeOOH and GR decreased with running time in both ARs, and the GR almost disappeared in the AR treated with O_3/Cl_2. Many studies had indicated that GR could be transformed to Fe_3O_4 and α-FeOOH, and α-FeOOH could also be transformed to Fe_3O_4 under anaerobic or anoxic conditions by the function of bacteria (Chaudhuri et al., 2001; Etique et al., 2014; Sun et al., 2014). The XRD results suggested that GR and α-FeOOH may be transformed to Fe_3O_4 in the corrosion scales, and more Fe_3O_4 and $CaCO_3$ were formed in AR treated with O_3/Cl_2.

In AR treated with Cl_2 alone, FESEM micrographs exhibited a predominant laminar structure for the corrosion scales at day 40 (Appendix A Fig. S5). From day 40 to day 170, the laminar structure became more compact. Zhu et al. (2014) had also indicated that the laminar structure of corrosion scales was easily formed in AR treated with Cl_2 disinfection. In AR treated with O_3/Cl_2, the corrosion scales showed globular tubercles structure at day 40. However, there were some pores on the surface of the corrosion products. From day 40 to day 170, the globular tubercles became thicker and more compact.

The above results indicated that the higher corrosion rate before day 40 in AR treated with O_3/Cl_2 induced the formation of globular tubercles. From day 40 to day 170, the increase of $CaCO_3$ content could decrease the porosity of the corrosion scales and induce the formation of compact tubercles (Wang et al., 2012c). Moreover, the iron phase composition of the globular tubercles was Fe_3O_4 and α-FeOOH. Many studies had indicated that the formation of Fe_3O_4 suggested the stable and compact corrosion scales formation (Yang et al., 2012; Jin et al., 2015; Sun et al., 2017), which could inhibit corrosion and iron release. Therefore, more stable corrosion scales were formed and iron release was lower in the AR treated with O_3/Cl_2.

2.3. Effects of biofilms on corrosion

The chemical parameters of water quality were the main factors which influenced the corrosion process in DWDSs (Yang et al., 2012). The main chemical parameters, including Cl^-, SO_4^{2-}, alkalinity, dissolved oxygen (DO) and pH, were measured in the influents of both ARs (Appendix A Table S4). There was no significant difference in water quality between the influents of both ARs ($p > 0.05$). However, the microbiologically influenced corrosion (MIC) also played a great role in stable corrosion scales formation (Sun et al., 2014; Wang et al., 2014; Jin et al., 2015). The iron-oxidizing bacteria (IOB) and iron-reducing bacteria (IRB) can influence the corrosion process and the composition of the corrosion scales. Therefore, the potential corrosive bacteria including IOB and IRB were identified using the most probable number (MPN) technique (Coby et al., 2011). The results showed that the abundance of IOB and IRB in the biofilms of corrosion scales in AR treated with O_3/Cl_2 disinfection was 1.2×10^9 and 4.5×10^7 cells/g corrosion scales, respectively, which was higher than that in the biofilms of AR treated with Cl_2 alone (Table 1).

After the MPN enumerations, the Fe(II) oxidation and Fe(III) reduction products caused by the bacteria in the biofilms of corrosion scales in AR treated with O_3/Cl_2 disinfection were measured using XRD. In AGW medium with 10 mmol/L $FeCl_2$, reddish-brown precipitates were formed. The main composition of the precipitates was α-FeOOH (Fig. 4), which came from the oxidation of Fe(II) by the bacteria in the biofilms of corrosion scales. In the AGW medium with 10-mmol/L synthetic hydrous ferric oxide, the color became black. The synthetic hydrous ferric oxide was amorphous, after the MPN experiment, Fe_3O_4, α-FeOOH and green rust were present (Fig. 4). This indicated that the bacteria in biofilms of corrosion scales could reduce Fe (III) to Fe(II). Because the MPN experiment showed the number of culturable Fe(III)-reducing and nitrate-dependent Fe(II)-oxidizing bacteria in the biofilms of corrosion scales, the results indicated that the biofilms indeed affected the corrosion process and composition of the corrosion scales.

Before day 40, the initial chlorine concentration and chlorine residual were not different between the both ARs. There was no difference in the corrosion process caused by chlorine reaction in both ARs. The higher corrosion rate and iron release may be caused by the higher contents of IOB in AR treated with O_3/Cl_2. The higher corrosion rate also drove the globular tubercles formation, causing the anaerobic or anoxic conditions formation in the corrosion scales where the dissolved oxygen could not reach (Jin et al., 2015). Therefore, the contents of IRB increased in the biofilms of both ARs. However, higher contents of IRB could favor transformation of the green rust and α-FeOOH to Fe_3O_4 (Sun et al., 2014; Jin et al., 2015; Wang et al., 2017). Therefore, the higher contents of IRB in AR treated with O_3/Cl_2 induced more Fe_3O_4 formation, which was also attributed to the formation of more stable and compact iron corrosion scales. Meanwhile, the stable and compact corrosion scales inhibited the iron release in AR treated with O_3/Cl_2.

Table 1 – Most probable number (MPN) enumerations of Fe(III)-reducing and nitrate-dependent Fe(II)-oxidizing bacteria in biofilms of corrosion scales in both annular reactors (ARs) at day 250.

Culture systems	Culture conditions	MPN (cells/g corrosion scales)		95% confidence interval	
		Cl_2	O_3/Cl_2	Cl_2	O_3/Cl_2
Fe(III)-reducing bacteria	Acetate + Fe(III)	2.5×10^7	4.5×10^7	3.6×10^6–1.3×10^8	7.1×10^6–2.4×10^8
Fe(II)-oxidizing bacteria	NO_3^- + Fe(II)	3.0×10^8	1.2×10^9	3.5×10^7–4.7×10^8	3.0×10^8–3.8×10^9

2.4. Effects of O_3/Cl_2 disinfection on opportunistic pathogens

Supply of safe drinking water is vital to public health. Opportunistic pathogens are recognized as one of the leading sources of waterborne disease outbreaks in developed countries (Wang et al., 2013). The bacteria in the effluents of distributed systems mainly came from the regrowth of bacteria in bulk water and the detachment of biofilms from the internal surface of pipes (Langmark et al., 2007; Liu et al., 2014). In order to control the opportunistic pathogens in the effluents and biofilm of DWDSs, O_3/Cl_2 disinfection was investigated in this study.

The stable corrosion scales had been formed in both ARs in the period from day 170 to day 250. During this period, 16S rRNA for total bacteria, three opportunistic pathogens (*L. pneumophila*, *M. avium* and *P. aeruginosa*), the broader genera (*Legionella* spp. and *Mycobacterium* spp.), and two amoeba hosts (*Acanthamoeba* spp. and *Naegleria* spp.), were detected in the influents, effluents and biofilms of different ARs by the qPCR method (Fig. 5). The results showed that the gene copy numbers of 16S rRNA in the influents of AR treated with O_3/Cl_2 was (2.19 ± 0.12) $\log_{10}$ (gene copies/mL), which was lower than that ((2.94 ± 0.13) $\log_{10}$ (gene copies/mL)) AR treated with Cl_2 alone (Fig. 5a). Moreover, no opportunistic pathogens were detected in the influents of AR treated with O_3/Cl_2, but *Mycobacteria* spp. at (0.61 ± 0.02) $\log_{10}$ (gene copies/mL) was detected in the influents of AR treated with Cl_2 alone.

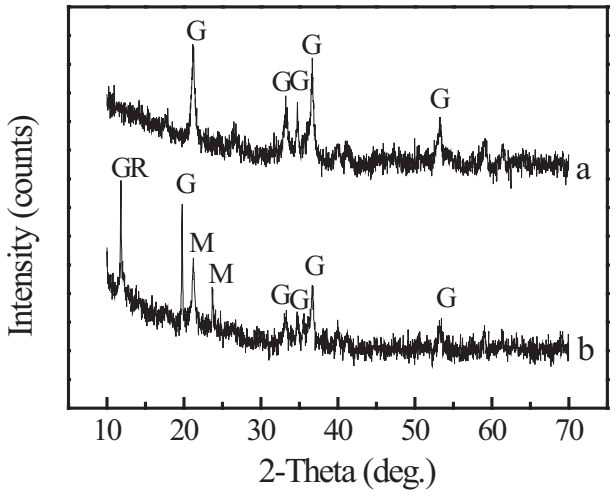

Fig. 4 – XRD patterns of the Fe(II) oxidation and Fe(III) reduction products resulting from the biofilms in the corrosion scales of AR treated with O_3/Cl_2 disinfection, (a) NO_3^- and $FeCl_2$, (b) synthetic hydrous ferric oxide. G: goethite, M: magnetite, GR: green rust.

The 16S rRNA gene copy numbers increased and different opportunistic pathogens occurred in effluents of both ARs (Fig. 5b). In effluents of AR treated with Cl_2 alone, the gene copy numbers of 16S rRNA, the opportunistic pathogens *P. aeruginosa*, *M. avium* and *L. pneumophila*, the broader genera *Mycobacterium* spp. and *Legionella* spp., and two amoeba hosts *Acanthamoeba* spp. and *Naegleria* spp. increased to (5.39 ± 0.31), (0.81 ± 0.03), (0.46 ± 0.02), (0.22 ± 0.02), (4.46 ± 0.122), (3.05 ± 0.12), (2.19 ± 0.12) and (0.12 ± 0.05) $\log_{10}$ (gene copies/mL), respectively. Compared with the AR treated with Cl_2 alone, the gene copy number of *P. aeruginosa* did not take great changes in effluents of AR treated with O_3/Cl_2 disinfection ($p > 0.05$). However, the gene copy numbers of *Mycobacterium* spp. and *Legionella* spp., and the amoeba *Acanthamoeba* spp. were lower in effluents of AR treated with O_3/Cl_2 disinfection than that AR treated with Cl_2 alone ($p < 0.05$). Moreover, the opportunistic pathogens *M. avium* and *L. pneumophila*, and the amoeba *Naegleria* spp. disappeared in the effluents of AR treated with O_3/Cl_2 disinfection.

In the biofilms of both ARs, the 16S rRNA for total bacteria and the opportunistic pathogens showed the same changes as these bacteria in effluents of both ARs (Fig. 5c). The gene copy numbers of 16S rRNA, the opportunistic pathogens *P. aeruginosa*, *M. avium* and *L. pneumophila*, the broader genera *Mycobacterium* spp. and *Legionella* spp., and two amoeba hosts *Acanthamoeba* spp. and *Naegleria* spp. increased to (11.3 ± 0.57), (5.57 ± 0.25), (5.39 ± 0.13), (3.60 ± 0.15), (9.78 ± 0.42), (8.93 ± 0.35), (8.37 ± 0.31) and (3.12 ± 0.06) $\log_{10}$ (gene copies/g corrosion scales), respectively, in biofilms of AR treated with Cl_2 alone. Except for *P. aeruginosa*, the 16S rRNA, opportunistic pathogens and the amoeba in the biofilms of AR treated with O_3/Cl_2 disinfection were all lower than that in AR treated with Cl_2 alone ($p < 0.05$). The gene copy numbers of the opportunistic pathogens *M. avium* and *L. pneumophila* decreased to (4.60 ± 0.14) and (3.09 ± 0.12) $\log_{10}$ (gene copies/g corrosion scales), respectively.

In the effluents and biofilms of both ARs, the gene copy numbers of the amoeba *Acanthamoeba* spp., the opportunistic pathogens *M. avium* and *L. pneumophila*, and the broader genera *Mycobacteria* spp. and *Legionella* spp. correlated very well ($r > 0.95$, $p < 0.05$). The results were consistent with other studies which have demonstrated that the opportunistic pathogens including *M. avium* and *L. pneumophila* could use amoebae such as *Acanthamoeba* spp. as a vehicle for protection and even replication (Delafont et al., 2014; Thomas et al., 2014). In particular, intracellular replication within an amoeba host was thought to be a prerequisite for *Legionella* spp. growth in oligotrophic environments (Wang et al., 2013; Declerck et al., 2009). The association between the amoeba and the opportunistic pathogens was contributed to the biofilms formation of

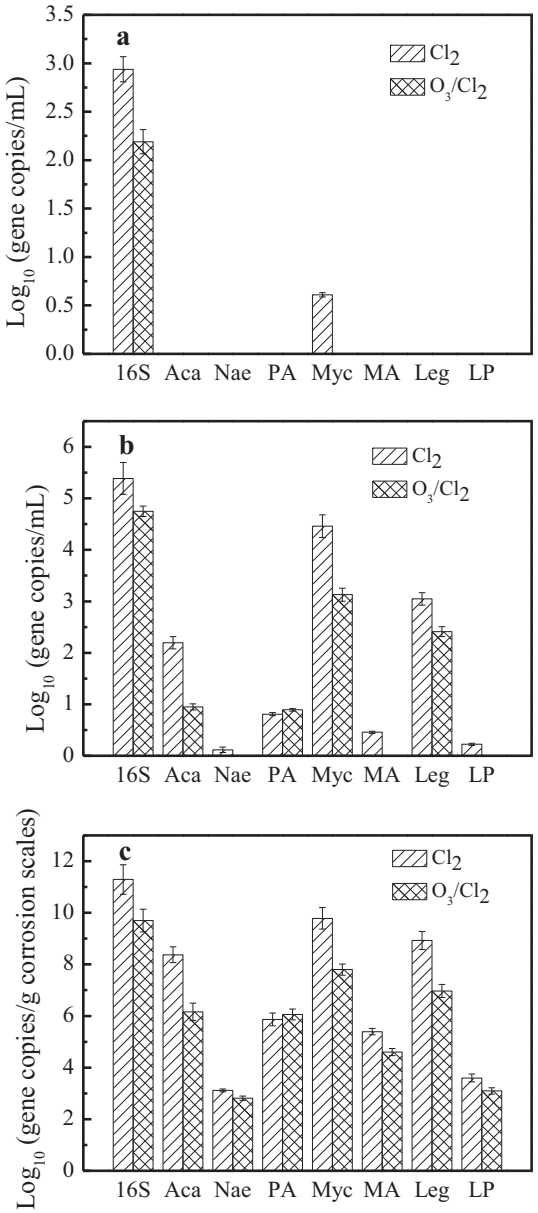

Fig. 5 – Quantitative polymerase chain reactions (qPCR) of 16S rRNA (16S) and different opportunistic pathogens in influents (a), effluents (b) and biofilms of corrosion scales (c) in both ARs. Error bars represent the standard deviation from the average of three replications. Aca: *Acanthamoeba* spp., Nae: *Naegleria* spp., PA: *Pseudomonas aeruginosa*, Myc: *Mycobacterium* spp., MA: *Mycobacterium avium*, Leg: *Legionella* spp., LP: *Legionella pneumophila*.

opportunistic pathogens and their resistance to disinfectants (Wang et al., 2013). Therefore, the association between the amoeba *Acanthamoeba* spp. and the opportunistic pathogens may be the reason for the higher amounts of these opportunistic pathogens in effluents and biofilms of AR treated with Cl_2 alone.

However, O_3/Cl_2 disinfection inactivated the amoebae and opportunistic pathogens effectively. In order to determine the effects of O_3 disinfection on control of the bacteria and opportunistic pathogens, the 16S rRNA for total bacteria and different opportunistic pathogens in raw water and the water after O_3 disinfection were also analyzed by the qPCR method (Fig. 6). The results showed that O_3 disinfection decreased the gene copy number of 16S rRNA for total bacteria from (5.95 ± 0.34) $\log_{10}$ (gene copies/mL) to (3.38 ± 0.29) $\log_{10}$ (gene copies/mL). Moreover, the opportunistic pathogen *P. aeruginosa*, and two amoeba hosts *Acanthamoeba* spp. and *Naegleria* spp. disappeared in the water after O_3 disinfection. The gene copy number of *Mycobacterium* spp. decreased from (2.63 ± 0.11) $\log_{10}$ (gene copies/mL) to (0.99 ± 0.12) $\log_{10}$ (gene copies/mL), and *Legionella* spp. decreased from (4.04 ± 0.35) $\log_{10}$ (gene copies/mL) to (1.67 ± 0.15) $\log_{10}$ (gene copies/mL). The results indicated that O_3 disinfection inactivated or damaged the amoebae and opportunistic pathogens effectively, due to its strong oxidizing properties and its ability to penetrate through the cell membrane according to other studies (Gunten, 2003; Alexander et al., 2016). The damaged bacteria resulting from O_3 disinfection such as *Mycobacterium* spp. and *Legionella* spp. can be inactivated efficiently by the subsequent chlorine disinfection. Therefore, *Mycobacterium* spp. and *Legionella* spp. were not detected in the influents of DWDSs treated with O_3/Cl_2 disinfection. Moreover, according to the chlorine residual results (Fig. 1), O_3 disinfection reduced the chlorine demand to control bacterial growth and biofilms formation in DWDSs, which also induced a higher chlorine residual in DWDSs treated with O_3/Cl_2 disinfection. Therefore, opportunistic pathogens *L. pneumophila* and *M. avium*, the broader genera *Legionella* spp. and *Mycobacteria* spp., and two amoeba hosts *Acanthamoeba* spp. and *Naegleria* spp. were all controlled in effluents and biofilms by O_3/Cl_2 disinfection.

3. Conclusions

The results indicated that O_3/Cl_2 disinfection affected the corrosion and iron release by changing the contents of IOB

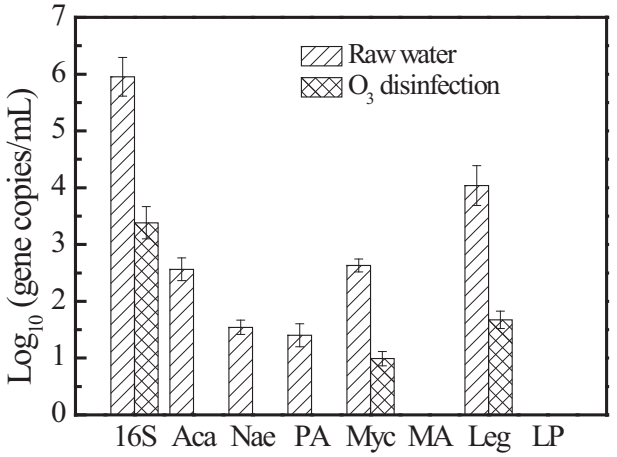

Fig. 6 – qPCR of 16S rRNA (16S) and different opportunistic pathogens in raw water and the water after O_3 disinfection. Error bars represent the standard deviation from the average of three replications. Aca: *Acanthamoeba* spp., Nae: *Naegleria* spp., PA: *Pseudomonas aeruginosa*, Myc: *Mycobacterium* spp., MA: *Mycobacterium avium*, Leg: *Legionella* spp., LP: *Legionella pneumophila*.

and IRB. The higher content of IOB in AR treated with O_3/Cl_2 may induce the higher corrosion rate in this AR before day 40. The higher corrosion rate drove the formation of globular tubercles, initiating higher content of IRB in the biofilms of corrosion scales from day 40 to day 170. Under this condition, more green rust and α-FeOOH were transformed to Fe_3O_4. The greater content of Fe_3O_4 and $CaCO_3$ induced the corrosion scales to be more stable, which inhibited the corrosion and iron release. Moreover, O_3/Cl_2 disinfection decreased the 16S rRNA for total bacteria to (2.19 ± 0.12) $\log_{10}$ (gene copies/mL) in the influents of AR obviously. The damaged bacteria resulting from ozone disinfection can be inactivated efficiently by the following chlorine disinfection. Therefore, the opportunistic pathogens *M. avium* and *L. pneumophila* disappeared in the effluents, and decreased to (4.60 ± 0.14) and (3.09 ± 0.12) $\log_{10}$ (gene copies/g corrosion scales) in biofilms, respectively. O_3/Cl_2 disinfection controlled the opportunistic pathogens in the effluents and biofilms of AR effectively.

Acknowledgments

This work was supported by the National Natural Science Foundation of China (No. 51290281) and the project of Chinese Academy of Sciences (No. QYZDY-SSW-DQC004) and the Federal Department of Chinese Water Control and Treatment (Nos. 2017ZX07108, 2017ZX07501002).

Appendix A. Supplementary data

Supplementary data to this article can be found online at https://doi.org/10.1016/j.jes.2018.01.009.

REFERENCES

Alexander, J., Knopp, G., Dotsch, A., Wieland, A., Schwartz, T., 2016. Ozone treatment of conditioned wastewater selects antibiotic resistance genes, opportunistic bacteria, and induce strong population shifts. Sci. Total Environ. 559, 103–112.

Berry, D., Xi, C., Raskin, L., 2006. Microbial ecology of drinking water distribution systems. Curr. Opin. Biotechnol. 17, 297–302.

Campese, C., Bitar, D., Jarraud, S., Maine, C., Forey, F., Etienne, J., et al., 2011. Progress in the surveillance and control of *Legionella* infection in France, 1998-2008. Int. J. Infect. Dis. 15, e30–e37.

Chaudhuri, S.K., Lack, J.G., Coates, J.D., 2001. Biogenic magnetite formation through anaerobic biooxidation of Fe(II). Appl. Environ. Microbiol. 67, 2844–2848.

Chiao, T.H., Clancy, T.M., Pinto, A., Xi, C., Raskin, L., 2014. Differential resistance of drinking water bacterial populations to monochloramine disinfection. Environ. Sci. Technol. 48, 4038–4047.

Cho, M., Chung, H., Yoon, J., 2003. Quantitative evaluation of the synergistic sequential inactivation of *Bacillus subtilis* spores with ozone followed by chlorine. Environ. Sci. Technol. 37, 22134–22138.

Coby, A.J., Picardal, F., Shelobolina, E., Xu, H.F., Roden, E.E., 2011. Repeated anaerobic microbial redox cycling of iron. Appl. Environ. Microbiol. 77, 6036–6042.

Corona-Vasquez, B., Samuelson, A., Rennecker, J.L., Marinas, B.J., 2002. Inactivation of *Cryptosporidium parvum oocysts* with ozone and free chlorine. Water Res. 36, 4053–4063.

Declerck, P., Behets, J., Margineanu, A., van Hoef, V., De Keersmaecker, B., Ollevier, F., 2009. Replication of *Legionella pneumophila* in biofilms of water distribution pipes. Microbiol. Res. 164, 593–603.

Delafont, V., Mougari, F., Cambau, E., Joyeux, M., Bouchon, D., Hechard, Y., Moulin, L., 2014. First evidence of amoebae-mycobacteria association in drinking water network. Environ. Sci. Technol. 48, 11872–11882.

EPA of China, 2002. Analysis Method for Water and Wastewater. Fourth ed. Press of Chinese, Environmental Science, Beijing.

Etique, M., Jorand, F.P.A., Zegeye, A., Gregoire, B., Despas, C., Ruby, C., 2014. Abiotic process for Fe(II) oxidation and green rust mineralization driven by a heterotrophic nitrate reducing bacteria (*Klebsiella mobilis*). Environ. Sci. Technol. 48, 3742–3751.

Gensberger, E.T., Polt, M., Konrad-Koszler, M., Kinner, P., Sessitsch, A., Kostic, T., 2014. Evaluation of quantitative PCR combined with PMA treatment for molecular assessment of microbial water quality. Water Res. 67, 367–376.

Gomez-Smith, C.K., LaPara, T.M., Hozalski, R.M., 2015. Sulfate reducing bacteria and mycobacteria dominate the biofilm communities in a chloraminated drinking water distribution system. Environ. Sci. Technol. 49, 8432–8440.

Gunten, U.V., 2003. Ozonation of drinking water: part II. Disinfection and by-product formation in presence of bromide, iodide or chlorine. Water Res. 37, 1469–1487.

Hwang, C., Ling, F., Andersenm, G.L., LeChevallier, M.W., Liu, W.T., 2012. Microbial community dynamics of an urban drinking water distribution system subjected to phases of chloramination and chlorination treatments. Appl. Environ. Microbiol. 78, 7856–7865.

Jin, J.T., Wu, G.X., Guan, Y.T., 2015. Effect of bacterial communities on the formation of cast iron corrosion tubercles in reclaimed water. Water Res. 71, 207–218.

Langmark, J., Storey, M.V., Ashbolt, N.J., Stenstrom, T.A., 2007. The effects of UV disinfection on distribution pipe biofilm growth and pathogen incidence within the greater Stockholm area, Sweden. Water Res. 41, 3327–3336.

Li, D., Li, Z., Yu, J., Cao, N., Liu, R., Yang, M., 2010. Characterization of bacterial community structure in a drinking water distribution system during an occurrence of red water. Appl. Environ. Microbiol. 76, 7171–7180.

Li, H.N., Zhu, X.P., Ni, J.R., 2011. Comparison of electrochemical method with ozonation, chlorination and monochloramination in drinking water disinfection. Electrochim. Acta 56, 9789–9796.

Liu, G., Bakker, G.L., Li, S., Vreeburg, J.H.G., Verberk, J.Q.J.C., Medema, G.J., et al., 2014. Pyrosequencing reveals bacterial communities in unchlorinated drinking water distribution system: an integral study of bulk water, suspended solids, loose deposits, and pipe wall biofilm. Environ. Sci. Technol. 48, 5467–5476.

Mi, Z., Dai, Y., Xie, S., Chen, C., Zhang, X., 2015. Impact of disinfection on drinking water biofilm bacterial community. J. Environ. Sci. 37, 200–205.

Miller, H.C., Wylie, J., Dejean, G., Kaksonen, A.H., Sutton, D., Braun, K., et al., 2015. Reduced efficiency of chlorine disinfection of *Naegleria fowleri* in a drinking water distribution biofilm. Environ. Sci. Technol. 49, 11125–11131.

Moradi, S., Liu, S., Chow, C.W.K., van Leeuwen, J., Cook, D., Drikas, M., et al., 2017. Developing a chloramines decay index to understand nitrification: a case study of two chloraminated drinking water distribution systems. J. Environ. Sci. 57, 170–179.

Morgan, M.J., Halstrom, S., Wylie, J.T., Walsh, T., Kaksonen, A.H., Sutton, D., et al., 2016. Characterization of a drinking water distribution pipeline terminally colonized by *Naegleria fowleri*. Environ. Sci. Technol. 50, 2890–2898.

Murphy, H.M., Payne, S.J., Gagnon, G.A., 2008. Sequential UV- and chlorine-based disinfection to mitigate *Escherichia coli* in drinking water biofilms. Water Res. 42, 2083–2092.

Sarin, P., Snoeyink, V.L., Bebee, J., Kriven, W.M., Clement, J.A., 2001. Physico-chemical characteristics of corrosion scales in old iron pipes. Water Res. 35, 2691–2697.

Sun, H.F., Shi, B.Y., Lytel, D.A., Bai, Y.H., Wang, D.S., 2014. Formation and release behavior of iron corrosion products under the influence of bacterial communities in a simulated water distribution system. Environ. Sci.: Processes Impacts 16, 576–585.

Sun, H.F., Shi, B.Y., Yang, F., Wang, D.S., 2017. Effects of sulfate on heavy metal release from iron corrosion scales in drinking water distribution system. Water Res. 114, 69–77.

Thomas, J.M., Ashbolt, N.J., 2011. Do free-living amoebae in treated drinking water systems present an emerging health risk? Environ. Sci. Technol. 45, 860–869.

Thomas, J.M., Thomas, T., Stuetz, R.M., Ashbolt, N.J., 2014. Your garden hose: a potential health risk due to *Legionella* spp. growth facilitated by free-living amoebae. Environ. Sci. Technol. 48, 10456–10464.

Wang, H., Edwards, M., Falkinham III, J.O., Pruden, A., 2012a. Molecular survey of the occurrence of *Legionella* spp., *Mycobacterium* spp., *Pseudomonas aeruginosa*, and *Amoeba* hosts in two chloraminated drinking water distribution systems. Appl. Environ. Microbiol. 78, 6285–6294.

Wang, H., Masters, S., Hong, Y., Stallings, J., Falkinham III, J.O., Edwards, M.A., et al., 2012b. Effect of disinfectant, water age, and pipe material on occurrence and persistence of *Legionella*, *mycobacteria*, *Pseudomonas aeruginosa*, and two amoebas. Environ. Sci. Technol. 46, 11566–11574.

Wang, H.B., Hu, C., Hu, X.X., Yang, M., Qu, J.H., 2012c. Effects of disinfectant and biofilm on the corrosion of cast iron pipes in a reclaimed water distribution system. Water Res. 46, 1070–1078.

Wang, H., Edwards, M.A., Falkinham III, J.O., Pruden, A., 2013. Probiotic approach to pathogen control in premise plumbing systems? A review. Environ. Sci. Technol. 47, 10117–10128.

Wang, H.B., Hu, C., Zhang, L.L., Li, X.X., Zhang, Y., Yang, M., 2014. Effects of microbial redox cycling of iron on cast iron pipe corrosion in drinking water distribution systems. Water Res. 65, 362–370.

Wang, H.B., Hu, C., Yin, L., Zhang, S.J., Liu, L.Z., 2017. Characterization of chemical composition and bacterial community of corrosion scales in different drinking water distribution systems. Environ. Sci.: Water Res. Technol. 3, 147–155.

Yang, F., Shi, B.Y., Gu, J.N., Wang, D.S., Yang, M., 2012. Morphological and physicochemical characteristics of iron corrosion scales formed under different water source histories in a drinking water distribution system. Water Res. 46, 5423–5433.

Zhang, S.H., Ye, C.S., Lin, H.R., Lv, L., Yu, X., 2015. UV disinfection induces a vbnc state in *Escherichia coli* and *pseudomonas aeruginosa*. Environ. Sci. Technol. 49, 1721–1728.

Zhu, Y., Wang, H.B., Li, X.X., Hu, C., Yang, M., Qu, J.H., 2014. Characterization of biofilm and corrosion of cast iron pipes in drinking water distribution system with UV/Cl2 disinfection. Water Res. 60, 174–181.